CONF-831174--76

CONF-831174--76

DE84 006664

ION-INDUCED SURFACE MODIFICATION OF ALLOYS*

by

H. Wiedersich

Materials Science and Technology Division
ARGONNE NATIONAL LABORATORY
Argonne, Illinois 60439

HW:po

Distribution:
1-3. M. F. Adams
4. B. R. T. Frost
5. L. C. Ianniello
6. Editorial Office
7. L. Rehn et al.
8. File

November 1983

INVITED PAPER to be presented at the Materials Research Society Annual Meeting, Boston, MA, November 14-17, 1983.

*Work supported by the Department of Energy.

ION-INDUCED SURFACE MODIFICATION OF ALLOYS*

H. Wiedersich, Argonne National Laboratory, 9700 South Cass Avenue, Argonne, IL 60439

ABSTRACT

In addition to the accumulation of the implanted species, a considerable number of processes can affect the composition of an alloy in the surface region during ion bombardment. Collisions of energetic ions with atoms of the alloy induce local rearrangement of atoms by displacements, replacement sequences and by spontaneous migration and recombination of defects within cascades. Point defects form clusters, voids, dislocation loops and networks. Preferential sputtering of elements changes the composition of the surface. At temperatures sufficient for thermal migration of point defects, radiation-enhanced diffusion promotes alloy component redistribution within and beyond the damage layer. Fluxes of interstitials and vacancies toward the surface and into the interior of the target induces fluxes of alloying elements leading to depth-dependent compositional changes. Moreover, Gibbsian surface segregation may affect the preferential loss of alloy components by sputtering when the kinetics of equilibration of the surface composition becomes competitive with the sputtering rate. Temperature, time, current density and ion energy can be used to influence the individual processes contributing to compositional changes and, thus, produce a rich variety of composition profiles near surfaces.

INTRODUCTION

Ion beam modification of alloy surfaces has become an active field of study during the past few years. The field has roots in several areas: ion implantation in semiconductors, radiation effects on the structure and properties of materials, effects of ion sputtering, and recognition of the potential to improve surface properties by ion beams. Recent conferences and books addressing these aspects of ion-solid interactions are cited in references [1-7]. The motivation for a large fraction of the work on alloys is the frequently beneficial effect of ion bombardment on technologically important properties and processes such as hardness, friction, wear, corrosion, catalysis, adhesion, and reflectance. Underlying these effects are ion-induced changes in microstructure, i.e., composition, phase distribution, crystal structure and defect microstructure, in the surface and the near surface regions of the material. It has become evident that a considerable number of distinct processes contribute to the evolution of the microstructure during ion bombardment, see e.g. [8]. Energetic ions cause rearrangement of atoms of the solid in displacement cascades, remove near surface atoms by sputtering and become incorporated into the material at the end of range. Disordering of atoms may transform the crystalline structure into an amorphous phase as is frequently observed in covalently bonded elements and compounds. Whereas most pure metals appear to remain crystalline during ion implantation even at low temperatures, alloys above a critical concentration are observed to become

*Work supported by the U.S. Department of Energy

amorphous, e.g., Al with $\geq$ 15 at.% Ni [9] and Mo with $\geq$ 20 at.% P [10]. Ordered alloys become disordered at sufficiently low temperatures; however, at temperatures at which point defects are mobile, the bombardment may accelerate the ordering reaction in partially ordered alloys. Excess interstitials and vacancies agglomerate in the form of dislocation loops and voids, leading to a complex defect microstructure near the implanted surface.

With the exception of the accumulation of the implanted species, the processes mentioned thus far can occur in the surface layer of a uniform alloy target without affecting the alloy component distribution. Several processes, however, initiate and maintain non-uniform distributions of alloying elements within the surface region during bombardment. Preferential loss of certain elements by sputtering reduces the concentration of those elements in the first few layers of the target. Gibbsian adsorption, in which the free energy of the surface is reduced by an increase in concentration of surface-active elements at the surface, leads to a preferential loss of surface-active elements even in the absence of true preferential sputtering. Defect fluxes from the damage region to the surface and toward the interior of the material may transport certain alloying components preferentially and, thus, produce a non-uniform concentration distribution. This process is termed radiation-induced segregation (RIS). Displacement mixing and radiation-enhanced and thermal diffusion counteract any non-uniform concentration distribution present prior to ion bombardment or induced by RIS or sputtering.

In this paper we give a short review of the mechanisms that have been found important in the development of alloy composition and microstructure near surfaces during ion bombardment, i.e., defect production and agglomeration, displacement mixing, radiation-enhanced diffusion, preferential sputtering, Gibbsian adsorption and radiation-induced segregation.

DEFECT PRODUCTION AND AGGLOMERATION

The development of the microstructure during ion bombardment at ion energies that result in ion ranges larger than the characteristic scale of the evolving microstructure is best treated by the concepts which have evolved in the radiation damage community. The scale ranges from a few nonometers at very low temperatures to tens of micrometers at high temperatures. We will concentrate in this section on the processes that occur in the "interior" of the damage range of the incoming ions, where the loss of defects and of alloying elements to the surface and to the undamaged region beyond the range is of minor consequence. For a conceptual understanding of the microstructural evolution of a material during ion bombardment, a treatment of the production and annihilation of defects and defect clusters by chemical rate theory is useful [see e.g. 11,12]. This theory assumes that defects are produced randomly at a density corresponding to the energy density deposited in nuclear collisions [see e.g. 13,14]. The defects are classified as "immobile", e.g., collapsed vacancy loops or void embryos, and potentially "mobile", e.g., interstitial atoms, vacancies, point defect-solute complexes and small clusters of point defects.

At temperatures sufficiently low so that neither interstitials nor vacancies migrate, the defect microstructure consists of displacement cascades which can be visualized as a core region from which atoms have been ejected to appear as interstitial atoms in the surrounding region. The severe rearrangement of atoms in the cascade may result in an amor-

strated in Fig. 1a for cascades produced by 100 keV Cu^+ ions in Cu_3Au taken from the work Black et al. [15]. Disordered regions occur at every cascade site. The vacancy rich regions collapse to dislocation loops in a fraction of the cascades as shown in Fig. 1b and 1c. With increasing dose, cascade regions overlap, and vacancy and interstitital type defects are created in close proximity of existing defects and defect clusters, so that spontaneous recombination of opposite defects occurs with increasing frequency. The material approaches a steady state when essentially each new defect is created within the recombination volume of an existing defect. The corresponding defect concentrations are expected to be $\lesssim 10^{-4}$ atom fraction. This recombination process will contribute to displacement mixing once cascade overlap becomes significant.

At temperatures where one defect type is mobile, the mobile defects annihilate at stationary defects and defect clusters, or form aggregates. In metals interstitials and small interstitial clusters usually become mobile at lower temperatures than vacancies. The ultimate steady state of the irradiated material in this temperature range will not be significantly different than that at lower temperatures, except that the density of the mobile species is greatly reduced, and that of the immobile species is correspondingly increased.

The steady state density of the less mobile defect starts to decrease from its low temperature limiting value when its thermal jump frequency becomes larger than the frequency of production of new defects within the recombination volume. The slow defect then samples a number of potential annihilation sites before a new defect is created in its recombination volume. As the temperature and, therefore, the jump frequency of the slow defects increase, their concentration decreases. Losses of mobile interstititals and vacancies occur by formation of immobile defect clusters, and by annihilation at stationary or slowly moving defect sinks. Frequently, interstitial dislocation loops grow by preferential absorption of

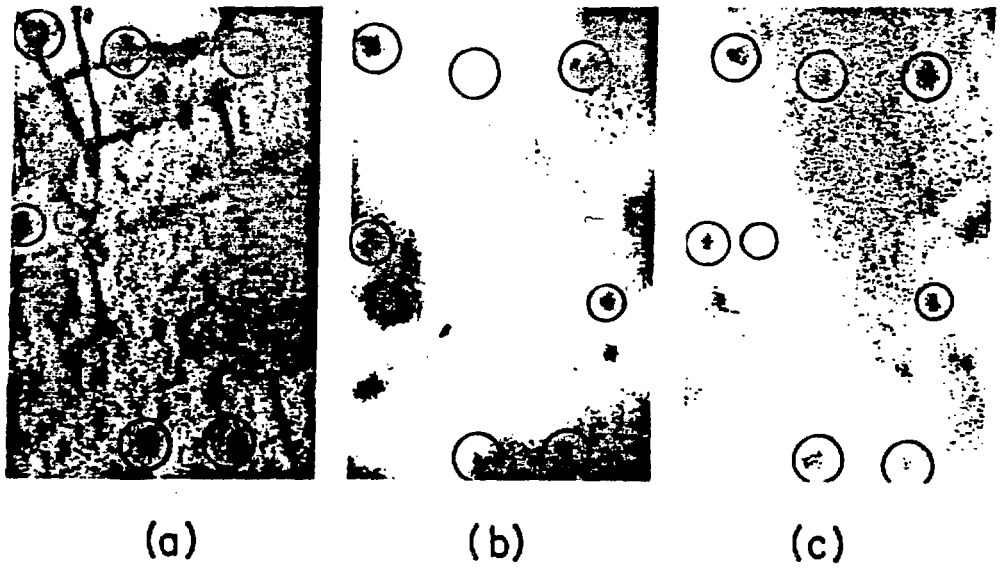

FIG. 1. Cascades produced in-situ by 100 keV Cu^+ in Cu_3Au and observed at low temperature: (a) (110) dark field superlattice image, showing disordered zones at cascade sites, (b) (220) dark field and (c) bright-field kinematical images showing loops at some cascade sites.

interstitials until they interact and form dislocation networks; vacancies preferentially agglomerate into voids. Defect annihilation at sinks induces defect concentration gradients and, hence, defect fluxes from the interior of crystalline regions to spatially discrete sinks. These fluxes, and the excess of mobile point defects are the predominant causes of microstructural developments of alloys during irradiation at elevated temperatures: radiation-induced and radiation-enhanced phase transformations, radiation-induced dislocation structures and void swelling [5,11,16].

Finally, at high temperatures little or no microstructural changes occur during irradiation. Defect clusters quickly decompose and high vacancy concentrations promote thermal annealing processes and eliminate long range migration of interstitials to sinks.

DISPLACEMENT MIXING AND RADIATION-ENHANCED DIFFUSION

Spatial redistribution of alloying elements requires diffusion or diffusion-like processes. As pointed out above, the production and annihilation of defects result in spatial relocation of atoms. We will use here the term "radiation-enhanced diffusion" for diffusion of elements under thermodynamic driving forces by thermally activated motion of defects during irradiation. The term "displacement mixing" will be used for the collection of processes which lead to redistribution of atoms without thermally activated defect motion. Cascade, ballistic and ion-beam mixing are frequently used instead of displacement mixing.

Several processes contribute to displacement mixing even though a precise distinction is sometimes difficult. Atoms are knocked off their original site and relocated. Relocation may also occur by replacement chains. Relaxation can also contribute to displacement mixing, e.g., by collapse of vacancy rich cascade cores. Extensive defect migration and defect recombination is expected during the "cooling phase" of high-energy-density cascades. Similarly, the high kinetic energy density during the evolution of a cascade will induce diffusion of preexisting defects. Finally, spontaneous recombination between preexisting and newly formed defects contributes to atomic mixing. A number of theoretical treatments for displacement mixing exist [17-21]. However, none includes all the processes mentioned.

A simple semi-empirical approach to describe displacement mixing follows along the suggestions of Anderson [17] and Matteson et al. [20]. Neglecting any anisotropy, the mixing process is considered as a random walk of atoms in three dimensions. The mean square distance, R^2, an atom has traveled after N uncorrelated jumps of length r_n is given by

$$R^2 = \sum_{n=1}^{N} r_n^2 \equiv N \langle r^2 \rangle \qquad (1)$$

where $\langle r^2 \rangle$ is the mean square length of the individual jumps. If the N jumps have taken place in a time interval t, one obtains the following relation between the diffusion coefficient D, the jump rate $N/t \equiv \nu$ and the mean square jump distance $\langle r^2 \rangle$ [22]

$$D = (1/6)\ \nu \langle r^2 \rangle. \qquad (2)$$

In this approximation, displacement mixing can be described by the usual diffusion formalism in a way very similar to thermal and radiation-enhanced diffusion. The quantities that must be estimated to apply eq. (2) are the rate with which atoms are changing sites, ν, and the mean square distance, $\langle r^2 \rangle$, associated with the site changes.

This task is especially simple for high temperature thermal diffusion in crystalline solids, where diffusion occurs by exchange of atoms with neighboring vacancies [22]. Therefore, we will discuss the application of eq. (2) to thermal and radiation-enhanced diffusion before returning to displacement mixing. Denoting the nearest neighbor distance by b, we have $\langle r^2 \rangle = b^2$ for atom-vacancy exchange. Neglecting all complications, such as correlation effects and solute-vacancy binding, the jump-frequency of an atom is the product of the probability of having a vacancy next to it, ZC_v, and the exchange frequency of the atom with the vacancy, ν_v; here C_v is the atomic fraction of vacancies and Z the coordination number. Thus,

$$D_{thermal} = (b^2/6)\, ZC_v\, \nu_v. \qquad (3)$$

Both ν_v and C_v contain Boltzmann factors with the activation enthalpy for migration and the formation enthalpy of vacancies, respectively. The straight line denoted "thermal" in the Arrhenius plot of the diffusion coefficient, Fig. 2, represents the thermal diffusion coefficient.

As discussed previously, the vacancy concentration is increased significantly above the thermal concentration at intermediate and low temperatures during ion bombardment, and diffusion of atoms via vacancies is described by eq. (3) with C_v representing the radiation-enhanced vacancy concentration. The presence and migration of interstitials during irradiation also contributes to diffusion. Hence, we can represent the diffusion coefficient during irradiation approximately as [24-26]

$$D_{rad} = (b^2/6)Z\, [C_v\, \nu_v + C_i\, \nu_i] \qquad (4)$$

where we have ignored potential differences in jump-distances and coordination numbers for intersititials and vacancies. The quantity in square brackets is calculated from rate theory [11, 12, 24]. At steady state, the contribution from the interstitials to D_{rad} equals that from the excess vacancies. The solid line in Fig. 2 is calculated for radiation conditions typical of high energy ion bombardment experiments.

The diffusion coefficient for displacement mixing is more difficult to estimate. The jump rate ν of atoms in eq. (2) should be proportional to the displacement rate, K. From molecular dynamics calculations King and Benedek found that ≈ 40 atoms change sites for each stable Frenkel pair produced at low primary recoil energies [27]. Similar numbers have been derived from experimentally determined disordering rates of ordered alloys at liquid He temperatures [28, 29]. The mean square jump distance $\langle r^2 \rangle$ should be a few times b^2, because a fraction of the atoms will be relocated by more than a nearest neighbor distance for larger recoil momenta in off-close-packed directions. Additional contributions to displacement mixing are expected from induced migration of preexisting defects and spontaneous defect recombination when cascade overlap becomes important. The diffusion coefficient due to displacement mixing can be written as

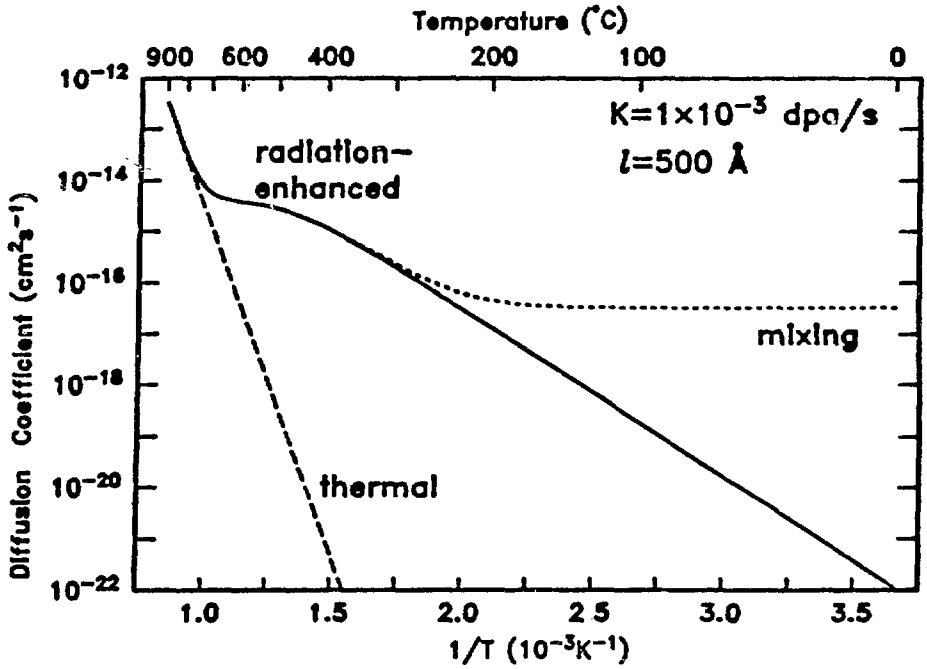

FIG. 2. The steady state diffusion coefficient in a 50 nm thick foil of Ni at a damage rate K = 10^{-3} dpa/s typical of ion bombardment, calculated from the analytical solution to the rate equations due to Lam et al. [23]. A sink density of $10^{10}/cm^2$ was assumed. The thermal diffusion coefficient and the diffusion coefficient due to displacement mixing (see text) are also shown.

$$D_{mix} = (b^2/6)\ \eta\ K \qquad (5)$$

where η should be on the order of 10^2 to 10^3 at steady state. Ion beam mixing of bilayer and of marker specimens at low temperature yield values for η in this range [30, 31]. The dotted line in Fig. 2 indicates the magnitude of mixing expected without thermally activated motion of defects at low temperatures. The diffusion coefficient from athermal mixing exceeds that expected from thermal motion of defects up to the temperature regime where vacancies become rather mobile.

PREFERENTIAL SPUTTERING AND GIBBSIAN ADSORPTION

Preferential loss of certain alloying elements from the surface induces compositional changes which spread into the interior by the diffusion processes discussed in the previous section. The yield or number of atoms of species i per incident ion in the flux of sputtered ions can be written as [8]

$$Y_i = \int_0^\infty p_i(x)\ C_i(x)\ dx = \bar{p}_i\ C_i^s \qquad (6)$$

where $p_i(x)$ is the probability per unit depth that an i-atom at depth $x > 0$ is ejected from the surface, $x = 0$, and $C_i(x)$ is the atomic fraction of i in the alloy at depth x. Written in this form, the distinction

between "true" preferential sputtering or primary effects and secondary effects in alloy sputtering is made explicit [31]. The sputter probability contains the physical variables that are directly related to the individual sputtering events, such as the type and energy of the incoming ion, the type of sputtered atom and its surface binding energy. Secondary effects, i.e., Gibbsian adsorption and radiation-induced segregation influence the yield because of their effects on the composition of the alloy in the near surface region.

The sputtered atoms come predominantly from a shallow surface layer [32]. For low energy sputtering the contributions fall off approximately exponentially with depth, with a decay length on the order of two atomic layers. Therefore, the integral in eq. (6) can be replaced to a good approximation by $\bar{p}_i \, C_i^s$ where $\bar{p}_i$ is the average total probability for an i-atom present in the surface layer to be sputtered off per incident ion and C_i^s is the average atomic concentration of i in the layer. The thickness of this layer is not well defined, but should be on the order of two atomic layers as recent results on high temperature sputtering of Ni-Cu alloys indicate [33].

The differences in the ejection probabilities, $\bar{p}$, for the component atoms of an alloy result primarily from differences (1) in the energy and momentum transferred to atoms of unlike masses in similar collisions with the same projectile, and (2) in the energy required by component atoms to overcome their specific surface binding energy. Anderson has recently given an extensive compilation and discussion of preferential sputtering in multicomponent metals [34].

Continuous sputtering of a semi-infinite alloy target of uniform bulk composition results eventually in a steady state in which the composition of the sputtered atom flux equals that of the bulk, i.e.,

$$Y_1 : Y_2 : Y_3 \ldots = C_1^b : C_2^b : C_3^b \ldots \qquad (7)$$

where Y_i and C_i^b are the yield and the atomic fraction in the bulk alloy of component i, respectively, of the element i. In addition, the sputtered flux contains the bombarding ion species corresponding to a yield of unity at steady state. Preferential sputtering is accommodated by an appropriate change in the near surface concentration at steady state. Combining the approximation given in eq. (6) with eq. (7) we obtain

$$(C_1^s/C_1^b) : (C_2^s/C_2^b) : (C_3^s/C_3^b) \ldots = 1/\bar{p}_1 : 1/\bar{p}_2 : 1/\bar{p}_3 \ldots \qquad (8)$$

i.e., the ratio of the surface and bulk concentrations of an element, at steady state, is inversely proportional to the sputter probability of that element. It should be emphasized that C_i^s is the concentration of i properly averaged over the depth of origin of sputtered atoms and, therefore, is heavily weighted towards the first few atom layers.

Whereas preferential sputtering tends to pin the surface concentration at a value different from the bulk value, see eq. (8), Gibbsian adsorption tends to minimize the surface free energy by increasing the concentration of surface-active elements in the outermost atom layer relative to that of deeper layers. When atom exchange by thermal or radiation-enhanced diffusion between the top and underlaying atom layers occurs rapidly enough compared to the sputtering rate, the concentration ratios

C_i^G/C_i will approach their thermal equilibrium values, e.g., in a binary alloy i, j [35]

$$C_i^G/C_i = C_j^G/C_j \exp (H_{ij}/kT) \quad (9)$$

where C^G and C are the atom fractions of i or j in the adsorption layer (~ 1 atom layer thick [36]) and the adjacent atom layer, respectively. H_{ij} is the enthalpy change resulting from the exchange between a j-atom in the surface and an i-atom in the adjacent atom layer, k the Boltzmann constant and T the absolute temperature. Enhanced loss of i will occur for $C_i^G/C_i > 1$, because the origin of sputtered atoms is heavily weighted towards the first atom layer. As a consequence, C_i in the subsurface layer will be reduced in an attempt to approach the equilibrium condition, eq. (9). We note that the thickness of the Gibbsian adsorption layer is expected to be smaller than the sputter depth [33]. Hence, the region for the proper averaging of C_i^s may include a portion of the depleted subsurface region.

Preferential loss of elements from the surface during sputtering leads, of course, to a corresponding subsurface depletion. At low temperature, the region of depletion will be spread out by displacement mixing only. With the estimate of D_{mix} given in the previous section and noting that the surface recession rate should be on the order of one atomic plane per dpa (displacement per atom), the altered layer thickness should be less than a few tens of atom layers for high energy ions, and not exceed the damage range for low energy ions.

At elevated temperatures radiation-enhanced and thermal diffusion can lead to significantly increased altered layer thicknesses [33,37]. This is especially noteworthy for the case of low energy ions typically used for sputtering. At temperatures at which the mobility of the slower defects is significant, vacancies and interstitials escape from the damage region. Hence, an increased diffusion coefficient extends far into the target. For example, the silicon depleted layers in Ni-Si alloys are 200 atom layers thick after prolonged sputtering with 5 keV Ar^+ ions at 700°C [38].

RADIATION-INDUCED SEGREGATION

Excess point defects produced by ion bombardment migrate thermally over significant distances at elevated temperature before being eliminated by recombination or annihilated at sinks such as surfaces, grain boundaries and dislocations. The spatial separation between defect production and annihilation leads to persistent defect fluxes, e.g., towards the surface, or from the peak damage region towards regions of lower defect production in front of and behind the peak damage region. Motion of defects requires motion of atoms, i.e., a vacancy exchanges sites with a neighboring atom, an interstitial atom jumps into an adjacent interstice, or interstitialcy motion forces a substitutional atom into an interstitial site while returning a different atom to a substitutional site. In alloys, defects will frequently migrate preferentially via atoms of some of the alloying components. This, in turn, will couple fluxes of alloying elements to defect fluxes. The combination of persistent defect fluxes and the preferential coupling of certain alloying elements to the defect fluxes leads to a non-uniform distribution of elements within the microstructure of an initially uniform alloy phase. This phenomenon of radiation-induced segregation (RIS) is rather common, and has been reviewed recently in some detail [39,40].

The underlying concepts are as follows. A flux of atoms of equal magnitude and direction is associated with interstitials, $J_a^i = J_i$. The flux of atoms induced by vacancies is also of the same magnitude, but opposite in direction to that of the vacancy flux, $J_a^v = -J_v$. Each of the atom fluxes can be proportioned among the components of the alloy identified by subscripts k,

$$J_a^i = \sum J_k^i = J_i \sum \alpha_k^i , \quad J_a^v = \sum J_k^v = J_v \sum \alpha_k^v \tag{10}$$

where α_k^i and α_k^v are the coupling constants between element k and the interstitital and the vacancy flux, respectively. A net flux of element k occurs unless $J_k^v = -J_k^i$, i.e., the vacancy-induced flux exactly compensates the interstitital-induced flux. At steady state with respect to defects, the flux of vacancies to sinks (or out of the peak damage region) equals that of interstitials, because both defects are produced in equal numbers, and recombination eliminates defects in equal numbers. This assures that the rate of the total number of atoms arriving at sinks or leaving the peak damage region quickly approaches zero; however, local compositional changes will still occur unless the coupling constants of each element to vacancies and interstitials are equal in magnitude and opposite in sign, $\alpha_k^v = -\alpha_k^i$.

Radiation-induced segregation has been established for numerous alloys [40]. It is most pronounced at intermediate temperatures, where defect mobilities are high. At lower temperatures, the high density of defect clusters which develops during bombardment suppresses long range migration of defects and, hence, segregation over significant distances. At high temperatures, high thermal diffusivities prevent the build-up of significant local concentration differences. In solid solution alloys, RIS frequently increases the local concentration of solute in the vicinity of defect sinks sufficiently to exceed the solubility limit. This is illustrated in the micrographs of Fig. 3, which shows the precipitation of Ni_3Si on several types of defect sinks during ion bombardment of a solid solution Ni-Si alloy.

Radiation-induced segregation can also lead to spatial redistribution of phases within the microstructure of polyphase alloys. For example, enrichment of the solvent (Ni) in the vicinity of defect sinks in the two-phase Ni-12.8 at. % Al alloy leads to the dissolution of Ni_3Al precipitates near the surface, grain boundaries and dislocation loops [41]. The complex redistribution of precipitates in the near surface region of a two-phase Ni-12.7 at. % Si alloy during ion bombardment at elevated temperature is illustrated in Fig. 4 which shows a cross section of the specimen from the surface to beyond the damage range [42]. Defect fluxes ending at the sample surface have deposited sufficient Si to form a continuous film of Ni_3Si on the surface. The Si originated, at least in part, just below the surface film as evidenced by a precipitate depleted zone. At the peak damage region, ~1 μm from the surface, the Ni_3Si precipitates have been entirely dissolved and a band of increased precipitate volume fraction has formed on either side of the peak damage region. Analysis by energy-dispersive x-ray spectroscopy has shown that the alloy in the peak damage region is almost entirely depleted of silicon, whereas the Si concentration in the precipitate depleted zone near the Ni_3Si surface film is close to the solubility limit.

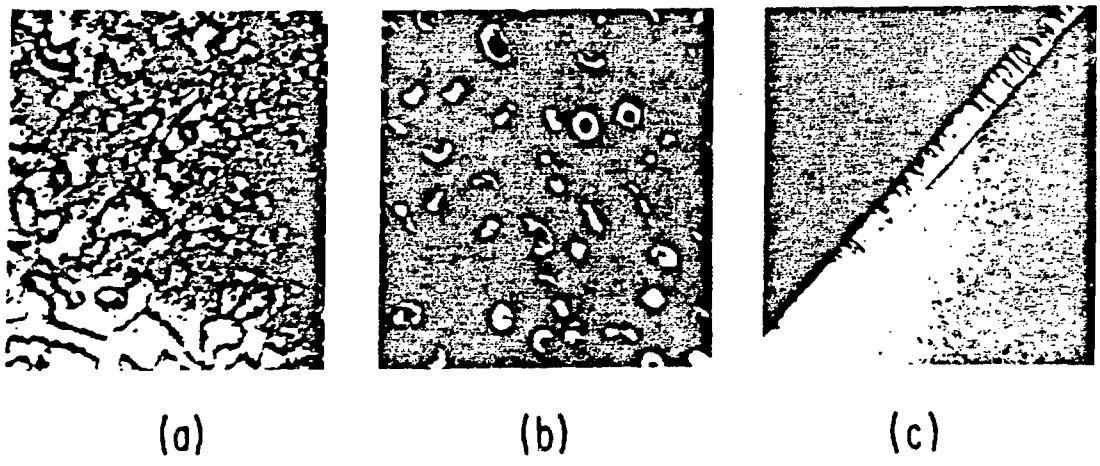

Fig. 3. Precipitation of Ni_3Si on defect sinks in solid solution Ni-Si alloys during irradiation; (a) the domain structure of the continuous surface film of Ni_3Si; (b) toroidal Ni_3Si precipitates that form on interstitial dislocation loops; (c) a Ni_3Si film that covers a grain boundary. Courtesy of P. R. Okamoto and K.-H. Robrock.

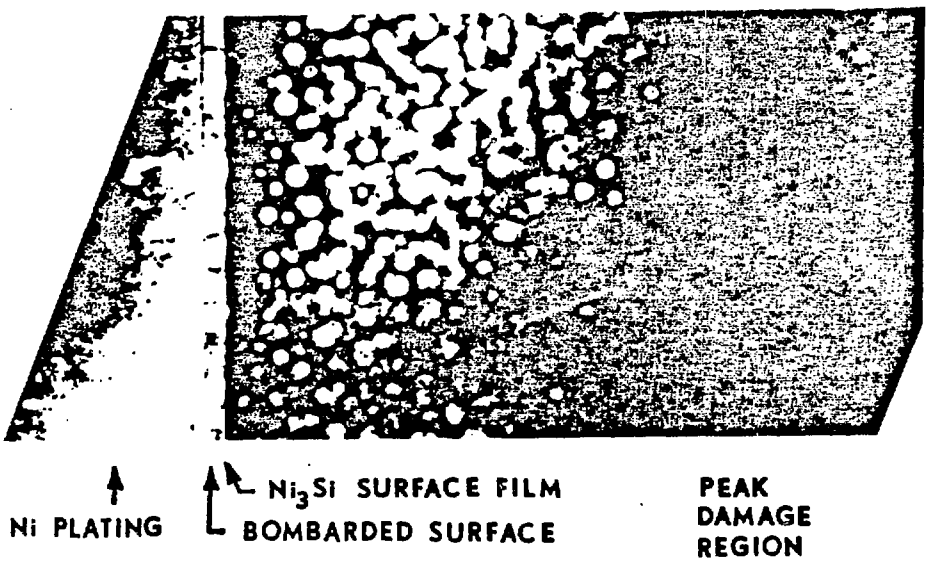

Fig. 4. Redistribution of Ni_3Si precipitates in a Ni-12.7 at. % Si alloy during bombardment with 250 keV protons at 500°C. Shown is a cross section prepared after plating the bombarded surface with Ni. The dark field image is produced by using a superlattice reflection of the Ni_3Si phase. The original uniformly distributed precipitate phase has formed a continuous film at the surface, depleting a subsurface layer of precipitates. The defect fluxes leaving the peak damage region removed most of the Si from this region. Courtesy of C. Allen, P. R. Okamoto and N. J. Zaluzec.

SUMMARY

Ion beams can modify the microstructure, composition and, hence, the properties of alloy surfaces in a variety of ways. The impact of the ions produces point defects and defect clusters. This process results in displacement mixing even at very low temperatures. It also may result in disordering of ordered alloys or amorphization. In materials that remain crystalline, a high density of defects and defect clusters develops with increasing dose at low temperatures. At intermediate temperatures, interstitial and vacancy defects become increasingly mobile, and the defect structures become less dense and well defined in the form of dislocation loops and networks, and, in many alloys, voids. With the reduced defect density, vacancies and interstitials migrate significant distances before annihilating at surfaces, dislocations and grain boundaries. The presence of excess mobile defects leads to radiation-enhanced diffusion, and the persistent defect fluxes lead to redistribution of alloy components and phases within and beyond the damage range. Selective loss of certain alloying elements by preferential sputtering and, indirectly, by Gibbsian adsorption or RIS and sputtering, leads to depletion of these elements from the near surface region. The depleted layer can spread significantly by displacement mixing, radiation-enhanced diffusion and RIS. It is evident that a wide variety of microstructures, and phase and composition distributions can be produced in near surface regions of alloys by appropriate choices of energy, type and current density of the bombarding ions, the irradiation temperature, and the initial structure and composition of the target.

Acknowledgements

Many stimulating discussions with my colleagues at ANL have contributed much to the integrated understanding of the processes contributing to the microstructural changes in ion bombarded surfaces described here. Special thanks go to L. E. Rehn for also critically commenting on the paper. M. A. O'Connor deserves acknowledgement for her able efforts to bring the manuscript into its final, pleasing appearance.

REFERENCES

1. R. E. Benenson, E. N. Kaufmann, G. L. Miller and W. W. Scholz, eds., Ion Beam Modifications of Materials (North-Holland, Amsterdam 1981); also see Nucl. Instrum. Methods 182/183, (1981).
2. B. Biasse, G. Destafanis and J. P. Gailliard, eds., Ion Beam Modifications of Materials (North-Holland, Amsterdam 1983); also see Nucl. Instrum. Methods 209/210 (1983).
3. J. M. Preece and J. K. Hirvonen, eds., Ion Implantation Metallurgy (TMS-AIME, New York 1980).
4. N. L. Peterson and S. D. Harkness, eds., Radiation Damage in Metals (American Society for Metals, Metals Park, Ohio 1976).
5. F. V. Nolfi, Jr., ed., Phase Transformations During Irradiation (Applied Science Publishers, London and New York, 1983).
6. J. M. Poate, G. Foti and D. C. Jacobson, eds., Surface Modification and Alloying by Laser, Ion and Electron Beams (Plenum Press, New York and London, 1983).
7. S. T. Picraux and W. J. Choyke, eds., Metastable Materials Formation by Ion Implantation (Elsevier Science Publishing Co., New York 1982).
8. H. Wiedersich, H. H. Anderson, N. Q. Lam, L. E. Rehn and H. W. Pickering, pp. 261-285 in Ref. 6.
9. S. T. Picraux and D. M. Follsteadt, in Ref. 6, pp. 287-321.
10. G. Linker, Nucl. Instrum. Methods 182/183, 501 (1981).

11. H. Wiedersich in Ref. 4, pp. 157-193.
12. A. D. Brailsford and R. Bullough, J. Nucl. Mater. 69 & 70, 434 (1978).
13. K. L. Merkle in Ref. 3, pp. 58-94; M. T. Robinson in Ref. 3, pp. 1-27.
14. J. A. Davies in Ref. 6, pp. 189-209.
15. T. J. Black, M. L. Jenkins and M. A. Kirk in: Proc. EMAG 83 (Electron Microscopy and Analysis Group - 1983), Guildford, England, August 1983, in press.
16. H. Wiedersich in: Advanced Techniques for Characterizing Microstructures, F. W. Wiffen and J. A. Spitznagel, eds. (AIME, New York 1982) pp. 15-30.
17. H. H. Anderson, Appl. Phys. 18, 131 (1979).
18. U. Littmark and H. O. Hofer, Nucl. Instrum. Methods 168, 329 (1980).
19. P. Sigmund and A. Gras-Marti, Nucl. Instrum. Methods 182/183, 25 (1981).
20. S. Matteson, B. M. Paine and M.-A. Nicolet, Nucl. Instrum. Methods 182/183, 53 (1981).
21. P. Sigmund, Appl. Phys. A30, 43 (1983).
22. P. G. Shewmon, Diffusion in Solids (McGraw-Hill, New York, 1963).
23. N. Q. Lam, S. J. Rothman and R. Sizmann, Radiat. Eff. 23, 53 (1974).
24. R. Sizmann, J. Nucl. Mater, 69/70, 386 (1968).
25. H. Wiedersich and N. Q. Lam, in Ref. 5, pp. 1-46.
26. S. J. Rothman, in Ref. 5, pp. 189-211.
27. W. E. King and R. Benedek, J. Nucl. Mater. 117, 26 (1983).
28. M. A. Kirk and T. H. Blewitt, Met. Trans. A9, 1729 (1978); also see J. Nucl. Mater. 108/109, 124 (1982).
29. R. H. Zee, M. W. Guinan and G. L. Kulcinski, J. Nucl. Mater. 114, 190 (1983).
30. R. S. Averback, L. J. Thompson and L. E. Rehn, these proceedings; also see S.-J. Kim, R. S. Averback, P. Baldo and M.-A. Nicolet, submitted to Appl. Phys. Lett.
31. P. Sigmund in: Sputtering by Particle Bombardment I, R. Behrish, ed., Topics in Applied Physics (Springer, Berlin 1981) pp. 11-71.
32. G. Falcone and P. Sigmund, Appl. Phys. 25, 307 (1981).
33. N. Q. Lam, H. A. Hoff, H. Wiedersich and L. E. Rehn, these proceedings.
34. H. H. Anderson in: Physics of Ionized Gases (SPIG 1980), M. Matić, ed. (Boris Kidric Institute of Nuclear Science, Beograd, Yugoslavia, 1980) p. 421.
35. P. Wynblatt and R. C. Ku in: Interfacial Segregation, W. C. Johnson and J. M. Blakely, eds. (American Society for Metals, Metals Park, Ohio 1979) p. 115.
36. Y. S. Ng, T. T. Tsong and S. B. McLane, Jr., Phys. Rev. Lett. 42, 588 (1979).
37. L. E. Rehn, N. Q. Lam and H. Wiedersich, these proceedings.
38. L. E. Rehn, V. T. Boccio and H. Wiedersich, Surface Sci. 128, 37 (1983).
39. H. Wiedersich and N. Q. Lam in Ref. 5, pp. 1-46.
40. L. E. Rehn and P. R. Okamoto in Ref. 5, pp. 237-290.
41. D. I. Potter in Ref. 5, pp. 213-245.
42. C. Allen, P. R. Okamoto and N. J. Zaluzec, to be published.